Steady-state two-level atomic population inversion via a quantized cavity field

Markus Lindberg and Craig M. Savage
Optical Sciences Center, University of Arizona, Tucson, Arizona 85721
(Received 7 June 1988)

A two-level atom illuminated by a laser may be driven into a population-inverted steady state if it is coupled to a cavity. This is a result of the quantum nature of the electromagnetic field and is forbidden by the semiclassical theory. We numerically and analytically analyze this inversion. We find the maximum possible inversion and determine the rate of approach to the steady state. The quantized cavity modifies the electromagnetic vacuum seen by the atom; this connects our work to that on cavity-enhanced spontaneous emission and on dynamical line narrowing. Experimental signatures of the inversion and potential experimental difficulties are considered. For example, neither the presence of many atoms in the mode nor many modes in the cavity destroys the inversion.

I. INTRODUCTION

Recently one of us (C.M.S.) predicted a new nonclassical effect of the interaction between a single two-level atom and a quantized cavity field:[1] The atomic population inversion can have positive values in the steady state. In this paper we study the mechanisms producing the inversion and explore its experimental implications.

Steady-state inversion is a consequence of the modification of the electromagnetic vacuum by the cavity. Thus it is related to cavity-enhanced and inhibited spontaneous emission,[2,3] and to dynamical suppression of spontaneous emission.[4] Other work on the interaction of a two-level atom with a quantized cavity includes Rice and Carmichael's[5] on nonclassical photon statistics and Savage and Carmichael's on single-atom optical bistability.[6]

In the semiclassical theory the electromagnetic field obeys Maxwell's classical dynamics and only the atom is quantized. A driven two-level atom in a cavity may be transiently inverted during Rabi oscillations, but steady-state inversion is semiclassically forbidden. However, when the field is quantized steady-state inversion becomes possible. The interaction between the electromagnetic field and atoms is known to show features that cannot be explained in semiclassical terms;[7] for example, squeezing[8] and antibunching.[9] These phenomena follow from small quantum fluctuations around the semiclassical steady state; therefore a linearized stochastic treatment is adequate. A shift of a semiclassical mean value, however, cannot happen in the usual linearized stochastic treatment;[10,11] a negative inversion remains negative in the presence of the small fluctuations treated by the linearized theory. Thus population inversion is, like quantum revivals of (collapsed) Rabi oscillations,[12] outside the usual linearized fluctuation regime of quantum optics. Work on superpositions of well-separated quantum field states by Yurke and Stoler,[13] Kennedy and Drummond,[14] and Wolinsky and Carmichael[15] also trancends the small-quantum-fluctuation regime.

The plan of this paper is as follows. Section II introduces our model and its associated master equation. From this the semiclassical theory is derived by making the usual factorization approximation. The numerical solution of the system's master equation is described in Sec. III. We present a parameter space survey of the positive inversion and show that it cannot exceed a certain small value. In Sec. IV we use truncation in the (vacuum picture) Fock state basis to obtain approximate, analytical solutions of the master equation. A connection to the Weisskopf-Wigner theory of spontaneous emission is established in Sec. V. Section VI deals with the experimental feasibility of positive inversion. We suggest exerimental signatures of inversion. Section VII is a summary of our results.

II. MODEL AND ITS PROPERTIES

The system under investigation consists of a single atom, inside a Fabry-Perot cavity, driven by a monochromatic laser beam, Fig. 1. Although it is difficult to faithfully represent all the details of such a system, the model we present contains the essential elements in the simplest possible way.

The dynamical participants in the system, the atom and the light field, are both treated quantum mechanically. The cavity naturally separates the light field into two parts; the vacuum field and the resonant cavity modes. We assume that the cavity-mode amplitude is linearly coupled to the external pump field amplitude. The model atom is a two-level system, assumed to be in exact resonance with the cavity mode. The interaction between the two-level system and the light field is treated in the dipole approximation using the Jaynes-Cummings interaction

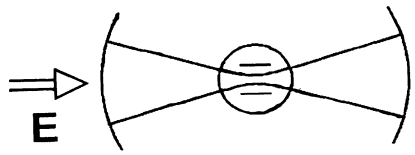

FIG. 1. Schematic diagram of the single atom in a cavity experimental setup. A laser of amplitude proportional to E drives the cavity.

Hamiltonian in the rotating-wave approximation. The essential dynamical effects of the vacuum modes are dissipation of the electronic excitation via spontaneous emission and damping of the resonant cavity-mode excitation, which we describe with the usual rates γ and κ, respectively.

With the assumptions made above the system obeys the following Liouville master equation for the atom-field density operator ρ:

$$\frac{d}{dt}\rho = L_{\rm af}(\rho) + L_f(\rho) + L_a(\rho) \ . \tag{2.1}$$

The first term is the Hamiltonian atom-field interaction,

$$L_{\rm af}(\rho) = g[a'^{\dagger}\sigma_- - a'\sigma_+, \rho] \ , \tag{2.2}$$

where a' ($a'^{\dagger}$) is the annihilation (creation) operator of the cavity mode, σ_- (σ_+) the lowering (raising) operator of the atomic levels, and g is the coupling constant, assumed to be real, and defined by

$$g = \left[\frac{3\pi\gamma c^3}{2\omega^2}\right]^{1/2} |\mathbf{u}(\mathbf{r})| \ , \tag{2.2a}$$

where γ is the spontaneous emission rate (Einstein-A coefficient), ω is the transition angular frequency, and c the speed of light. $\mathbf{u}(\mathbf{r})$ is the normalized cavity-mode function at the atomic position $\mathbf{r}$ (see Sec. VI). We also introduce the atomic inversion operator $\Delta\hat{p}$,

$$\Delta\hat{p} = \sigma_+\sigma_- - \sigma_-\sigma_+ \ . \tag{2.3}$$

The expectation value of this operator, $\langle \Delta\hat{p} \rangle$, is the population difference between the excited and ground atomic states. The second term in Eq. (2.1) describes the pumping and decay of the cavity mode,

$$L_f(\rho) = E[a'^{\dagger} - a', \rho] + \kappa(2a'\rho a'^{\dagger} - a'^{\dagger}a'\rho - \rho a'^{\dagger}a') \ . \tag{2.4}$$

The linear coupling of the pump-field amplitude with the cavity-mode amplitude is characterized by the constant E which is proportional to the pump-field amplitude. The cavity decay rate is 2κ. The last term in the master Eq. (2.1) describes atomic spontaneous emission and has the form

$$L_a(\rho) = (\gamma/2)(2\sigma_-\rho\sigma_+ - \sigma_+\sigma_-\rho - \rho\sigma_+\sigma_-) \ . \tag{2.5}$$

In the absence of the atomic interaction the steady-state field is the pure coherent state, $\rho = |E/\kappa\rangle\langle E/\kappa|$. We transform away the empty cavity (classical) field by dividing the field operator into a classical and a quantum part,

$$a' \equiv \frac{E}{\kappa} + a \ . \tag{2.6}$$

The new operator a obeys the same boson algebra as a'; this transformation takes us into the so-called vacuum picture.[16] The atomic expectation values are not influenced by this transformation. Instead of the field pumping term the transformed equations of motion have a semiclassical atom-field interaction

$$L_{\rm af}(\rho) \rightarrow \frac{gE}{\kappa}[\sigma_- - \sigma_+, \rho] + g[a^{\dagger}\sigma_- - a\sigma_+, \rho] \ , \tag{2.7}$$

$$L_f(\rho) \rightarrow \kappa(2a\rho a^{\dagger} - a^{\dagger}a\rho - \rho a^{\dagger}a) \ . \tag{2.8}$$

The Liouvilleans (2.5), (2.7), and (2.8) are used in the actual calculations performed in the rest of this paper. In Fig. 2 we show the state structure and the interactions between the states for the first two (transformed) Fock states.

In the case of many nearly degenerate cavity modes, of which only one is coupled to the external field, we can still use the equations for a single cavity mode, but with scaled parameters. We restrict ourselves to equal cavity dampings κ and equal coupling g of each mode with the atom. By performing an orthogonal transformation on the modes a new set can be found such that only one mode couples to the atom. All the new modes have the same cavity damping as the old ones. Hence only the coupled mode survives in the steady state, the others are damped to extinction. However, the effective atom-field coupling constant g is scaled by the number of modes N_m,

$$\beta \equiv gE/\kappa \rightarrow \beta, \quad g \rightarrow \sqrt{N_m}g, \quad \kappa \rightarrow \kappa \ . \tag{2.9}$$

Therefore the results of this paper can be used in the degenerate multimode case.[2]

In order to compare quantum-mechanical results concerning the atomic inversion with the semiclassical results, we briefly consider the semiclassical model. The semiclassical theory assumes that the atomic and light field degrees of freedom are separate and neglects higher-order coherences between the atomic and field variables. Specifically, expectation values containing atomic and field operators are assumed to factorize, which is equivalent to assuming that the density matrix is a direct product of the form

$$\rho = \rho_{\rm atom} \otimes \rho_{\rm field} \ . \tag{2.10}$$

Using the untransformed Liouvilleans (2.2), (2.4), and (2.5), we find the following equations of motion for the

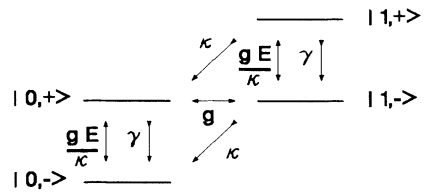

FIG. 2. State structure for two Fock state truncation. Arrows indicate possible directions of population movement. The arrow labels correspond to terms in Eqs. (2.5), (2.7), and (2.8).

expectation values $\langle a' \rangle = E/\kappa + \langle a \rangle$ and $\langle \Delta\hat{p} \rangle$:

$$\frac{d}{dt}\langle a' \rangle = E - \kappa\langle a' \rangle + g\langle \sigma_- \rangle , \tag{2.11}$$

$$\frac{d}{dt}\langle \sigma_- \rangle = -\gamma/2\langle \sigma_- \rangle + g\langle a'\Delta\hat{p} \rangle \cong -\gamma/2\langle \sigma_- \rangle + g\langle a' \rangle\langle \Delta\hat{p} \rangle , \tag{2.12}$$

$$\frac{d}{dt}\langle \Delta\hat{p} \rangle = -\gamma(\langle \Delta\hat{p} \rangle + 1) - 2g\langle a'^{\dagger}\sigma_- \rangle - 2g\langle \sigma_+ a' \rangle \cong -\gamma(\langle \Delta\hat{p} \rangle + 1) - 2g\langle a'^{\dagger} \rangle\langle \sigma_- \rangle - 2g\langle \sigma_+ \rangle\langle a' \rangle . \tag{2.13}$$

The steady state inversion is then

$$\langle \Delta\hat{p} \rangle \equiv \Delta p = -\frac{1}{1 + \frac{8g^2 |\langle a' \rangle|^2}{\gamma^2}} < 0 . \tag{2.14}$$

Hence the semiclassical inversion cannot be positive. However, nothing prevents positive inversion when the semiclassical approximation, Eq. (2.10), breaks down.

If the driving is done through a cavity mirror, as we assume for our discussion, this system can yield absorptive optical bistability in the semiclassical limit. However, when the photon number in the cavity is low, semiclassical bistability is destroyed by the quantum mechanics.[5,6] The saturation photon number n_s, naturally determined by Eq. (2.14), and other dimensionless parameters characterizing the semiclassical theory are defined by

$$n_s = \frac{\gamma^2}{8g^2}, \quad C = \frac{g^2}{\kappa\gamma}, \quad Y = n_s^{-1/2}\frac{E}{\kappa} . \tag{2.15}$$

The inverse relations are

$$g/\kappa = (8n_s)^{1/2}C, \quad \gamma/\kappa = 8n_s C, \quad E/\kappa = Yn_s^{1/2} . \tag{2.16}$$

We are interested in parameter regimes where the quantum-mechanical corrections to the population inversion are dominant, i.e., the semiclassical inversion is zero. From the semiclassical theory we expect the spontaneous emission to decrease the inversion towards $\Delta p = -1$. When the spontaneous emission rate γ is the slowest rate one might expect the inversion to be saturated to zero. However, this is not in general the case. The cavity damping provides an additional spontaneous decay channel, called cavity-enhanced spontaneous emission, with the route

$$|n,+\rangle \rightarrow |n+1,-\rangle \rightarrow |n,-\rangle ,$$

where $|n,\pm\rangle$ is the product of a field Fock state $|n\rangle$ and the atomic ground or excited state. The first step of this route is made by the quantum-mechanical atom-field coupling and the second step by the cavity damping (see Fig. 2). This rate may be estimated to be g^2/κ when $g \ll \kappa$ [Sec. IV B]. In order to keep the system saturated this rate and the spontaneous emission rate must be small in comparison with the Rabi frequency 2β; $\gamma, g^2/\kappa \ll \beta$. These conditions are met if

$$\gamma, g \ll \kappa, \beta . \tag{2.17}$$

The condition stated by Eq. (2.17) means that the quantum-mechanical coupling between the atom and the field is weak. The quantum part of the field then automatically cascades towards low quantum numbers where fluctuations can be large in comparison to the large quantum-number region. If, however, $g \ll \gamma$ the system collapses into the zero photon state, which is a pure semiclassical two-level system. To have essential quantum effects we must, hence, be in the region where

$$\gamma \ll g . \tag{2.18}$$

Indeed, as shown in Sec. III, when Eqs. (2.17) and (2.18) are fulfilled we obtain positive inversion in the steady state.

III. NUMERICAL RESULTS

The parameters $C = 1$, $n_s = 0.01$ ($g/\kappa = 0.28$, $\gamma/\kappa = 0.08$) satisfy the inequalities (2.17) and (2.18). Figure 3 plots the resulting inversion as a function of driving field Y. Positive inversion first occurs for $Y \cong 12$ ($\beta/\kappa \cong 3.4$). In Sec. VI we suggest that the local maximum of the inversion, shown in Fig. 3, is a signature of positive inversion. We have calculated the inversion, maximized with respect to the driving field, as a function of C and n_s. The results are shown in Fig. 4 as contours of the inversion Δp in the C, n_s plane. The maximum inversion for $C \in [0,5]$ and $n_s \in [0,0.001]$ is a little over 0.045.

What is the maximum possible inversion? In Fig. 4 the maximum occurs for small n_s and large C. The limit $n_s \rightarrow 0$ with $C(8n_s)^{1/2} = g/\kappa$ constant, is the limit of zero spontaneous emission, $\gamma \rightarrow 0$. It is physically reasonable that the largest inversion should occur for zero spontaneous emission. For $\gamma = 0$ we have numerically maximized the inversion with respect to the two remaining parameters: g and E. The resulting maximum inversion $\Delta p_{\max} = 0.070$ occurs for $g/\kappa = 1.2$ and $E/\kappa = 1.63$. This is a physical upper limit to the steady-state inversion in our model.

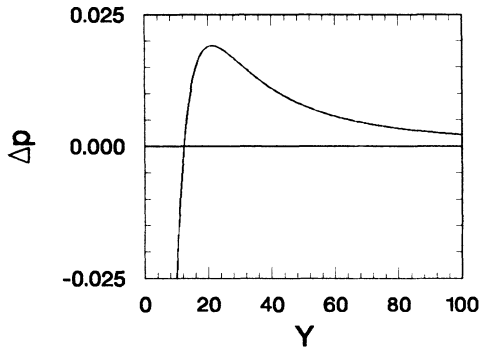

FIG. 3. Graph of the inversion Δp vs the cavity driving field Y. The maximum of the inversion occurring for $Y = 20$ corresponds to a maximum of the fluorescence as a function of driving field. This is a signature of positive inversion. Parameters: $C = 1$, $n_s = 0.01$ ($g/\kappa = 0.28$, $\gamma/\kappa = 0.08$).

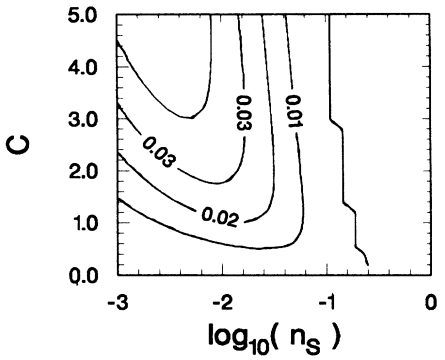

FIG. 4. Contour plot of the inversion, maximized with respect to the driving field, vs $\log_{10}(n_s)$ and C. For given C and n_s the contours indicate the maximum inversion obtainable by varying the driving field Y. For example, the parameters $C=2$ and $n_s=10^{-2}$ yield a maximum inversion Δp of about 0.03. In the region to the right of the rightmost contour (the zero contour) the inversion is always negative.

Next we compare our numerical results with the predictions of the one-atom semiclassical theory (Sec. II) and of Rice and Carmichael.[5] They find in their bad cavity limit,

$$\kappa/\gamma\rightarrow\infty,\quad n_s\rightarrow 0,\quad E/\kappa\rightarrow 0; C, Y \text{ constant} \tag{3.1}$$

that the inversion is given by

$$\Delta p=-\frac{(1+2C)^2}{(1+2C)^2+Y^2}\ . \tag{3.2}$$

The factors of $(1+2C)^2$ in this expression are the result of cavity-enhanced spontaneous emission. Figure 5 shows that both the semiclassical and the bad-cavity-limit approximations break down before positive inversion occurs.

The semiclassical theory should be valid when there are a large number of atoms in the cavity. Does positive inversion vanish as the number of atoms increases? We have investigated this question using the relevant generalization of the master equation (2.1) to N_A atoms.[11] For each atom a new Jaynes-Cummings interaction and a new spontaneous emission term is added.

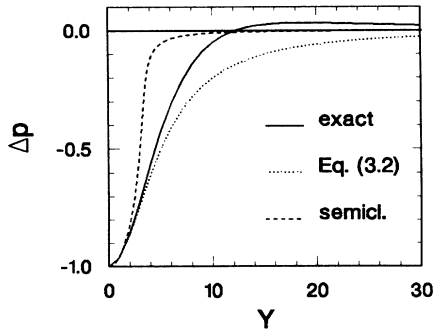

FIG. 5. Graphs of the inversion Δp vs the driving field Y from the exact numerical calculations (solid line), the semiclassical theory (dashed line), and the theory of Rice and Carmichael (Ref. 5) (dotted line). Parameters: $C=2$, $n_s=0.01$ ($g/\kappa=0.57$, $\gamma/\kappa=0.16$).

Solving for the inversion as a function of driving field we find the results shown in Fig. 6. As the number of atoms increases the maximum inversion decreases, and it occurs for larger driving fields. With five atoms in the cavity the maximum inversion per atom is $\Delta p=0.025$, compared with the maximum inversion for one atom, $\Delta p=0.032$, with the same parameters.

Also shown in Fig. 6(a) are the semiclassical predictions for Δp versus driving field. (For saturation photon numbers less than 1, such as we have here, any bistable behavior is expected to be completely washed out by quantum fluctuations.[5,6]) Agreement is good for small driving fields and improves as the number of atoms increases. For large driving fields both the semiclassical and quantum results saturate to zero. With five atoms the exact result agrees well with the lower branch of the semiclassical result.

We next discuss the numerical methods used to obtain the preceding results. After choosing a particular atom-field basis the master equation (2.1) may be represented by a linear system of ordinary differential equations, of infinite order. However, if the system contains only a small number of energy quanta it may be truncated to a

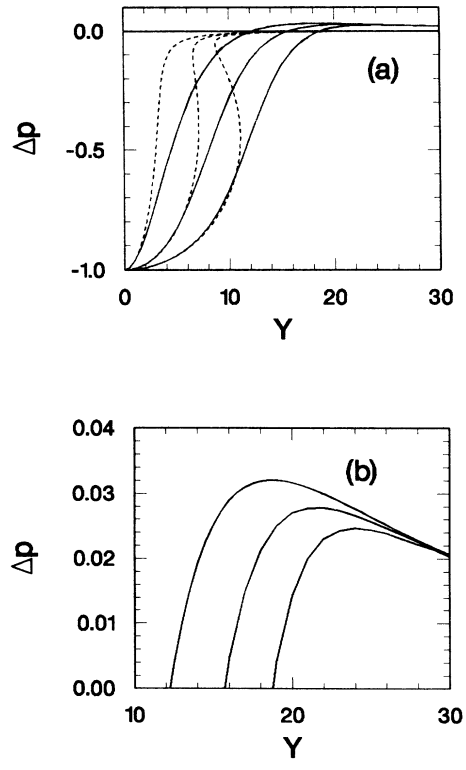

FIG. 6. Graphs of the inversion per atom Δp vs Y for different numbers of atoms in the cavity. From left to right the three sets of curves correspond to one atom, three atoms, and five atoms. Parameters: $C=2$, $n_s=0.01$ ($g/\kappa=0.57$, $\gamma/\kappa=0.16$). (a) The solid curves are exact numerical results, while the dashed curves are the semiclassical predictions. (b) Close up of positive inversion region showing convergence of all three curves for large driving fields.

correspondingly small-order system. This allows a numerical solution.

We choose our basis to be the tensor product of the field Fock states $|n\rangle$ and the atomic ground state $|-\rangle$ and excited state $|+\rangle$,

$$\{|+,n\rangle \equiv |+\rangle \otimes |n\rangle, \quad |-,n\rangle \equiv |-\rangle \otimes |n\rangle ; \quad n=0,1,2,\ldots\} . \tag{3.3}$$

Making the transformation of Eq. (2.6) significantly reduces the number of Fock states required in the problem because we do not need to represent the coherent state "tail." The empty cavity part of the field, the coherent state $|E/\kappa\rangle$, is transformed into the vacuum state.

The steady state of the master equation (2.1) is now found by solving the truncated linear system for the density-matrix elements. An inhomogeneous equation for the diagonal sum, corresponding to the normalization of the trace of the density matrix equal to one, must first be substituted into the system.

The accuracy of the solution in the truncated basis was checked by increasing the number of Fock states and demanding no change in the density-matrix elements. Table I shows the results of a typical steady-state solution obtained after a truncation to six Fock states. Taking into account the symmetry of the density matrix, 78 real density-matrix elements were solved for. Numerically this presented no problem.

When we have more than one atom coupled to the mode the problem becomes too large for standard linear equation solvers. With N_A atoms and N Fock states the total number of states in the truncated basis is $2^{N_A}\times N$. For example, five atoms and five Fock states gives a total of 160 basis states and $80\times 161=13{,}480$ density-matrix elements. Such a large linear system may be solved by the method described by Savage and Carmichael:[6] The master equation (2.1) may be expressed in the form

$$\frac{d\rho}{dt}=\mathbf{L}\rho , \tag{3.4}$$

where the density matrix ρ is represented as a vector ρ, using some arbitrary ordering of the density-matrix elements. This system of linear, ordinary, differential equations may be solved by the one step Euler method,

$$\rho(t)\rightarrow[\mathbf{I}+(t/k)\mathbf{L}]^k\rho(0), \quad k\rightarrow\infty . \tag{3.5}$$

The steady state is the long time solution. $\mathbf{L}$ is a sparse matrix having at most $2+5N_A$ nonzero elements per row. For large numbers of atoms the number of density-matrix elements required may be greatly reduced by using the atomic permutation symmetries.[17] For arbitrarily large numbers of atoms the Langevin equation method described by Smith and Gardiner is appropriate.[18]

TABLE I. Steady-state, diagonal, and vacuum-picture density-matrix elements in the basis of field Fock states and atomic eigenstates of Δp. Parameters are $C=2$, $n_s=0.01$, and $Y=20$. The column sums show an excess of population in the excited atomic state.

n	$\langle n,-\|\rho_v\|n,-\rangle$	$\langle n,+\|\rho_v\|n,+\rangle$	$\langle n,-\|\rho_v\|n,-\rangle$ $+\langle n,+\|\rho_v\|n,+\rangle$
0	0.423	0.485	0.908
1	0.058	0.030	0.088
2	0.003	6×10^{-4}	0.004
3	5×10^{-5}	5×10^{-6}	$<10^{-4}$
4	4×10^{-7}	2×10^{-8}	$<10^{-6}$
5	1×10^{-9}	6×10^{-11}	$<10^{-8}$
Sum	0.484	0.516	1

IV. ANALYTICAL RESULTS

A. Positive inversion

The model described in Sec. II can be solved approximately in certain limits. A positive inversion is obtained when the classical part of the field is large enough to totally saturate the atomic transition. The quantum-mechanical effects are then able to raise the inversion to a positive value. We analytically evaluate the theory in the limit when the quantum-mechanical field coupling is weak compared to the cavity damping. This does not mean that we can neglect the small coupling. In the neighborhood of the zero photon states the small coupling measured by g becomes important, as discussed in Sec. II. We now assume that $g\ll\kappa$. Because g measures the only process which takes the system upwards in the photon states, the system automatically cascades towards the lower photon numbers. In this limit the truncation of the photon state basis to the $|0\rangle$ and $|1\rangle$ Fock states is a natural approximation. One should, however, bear in mind that due to our transformation to the vacuum picture we are talking about photons "on top" of the coherent state $|E/\kappa\rangle$. This approximation is not equivalent to a perturbation expansion in g if $\beta<g$.

The set of equations we have to solve is then

$$\frac{d}{dt}\rho(0,0)=\beta[\sigma_- -\sigma_+,\rho(0,0)]+L_a(\rho(0,0)) -g[\rho(0,1)\sigma_- +\sigma_+\rho(1,0)]+2\kappa\rho(1,1) , \tag{4.1}$$

$$\frac{d}{dt}\rho(1,1)=\beta[\sigma_- -\sigma_+,\rho(1,1)]+L_a(\rho(1,1)) +g[\sigma_-\rho(0,1)+\rho(1,0)\sigma_+]-2\kappa\rho(1,1) , \tag{4.2}$$

$$\frac{d}{dt}\rho(1,0)=\beta[\sigma_- -\sigma_+,\rho(1,0)]+L_a(\rho(1,0)) +g[\sigma_-\rho(0,0)-\rho(1,1)\sigma_-]-\kappa\rho(1,0) , \tag{4.3}$$

$$\rho(0,1)=\rho(1,0)^\dagger . \tag{4.4}$$

where $\beta=gE/\kappa$. The form of the spontaneous emission part, L_a, is given by Eq. (2.5). The notation used is simply

$$\langle 0|\rho|0\rangle\equiv\rho(0,0), \quad \text{etc.} ,$$

where the matrix elements are taken in the photon Fock

states. Hence the "matrix elements" are still operators on the atomic states.

To solve Eqs. (4.1)–(4.4) is straightforward but tedious and we do not go into the details of it. We are interested in the total atomic inversion, which is given by

$$\Delta p = \langle + | \rho(0,0) | + \rangle + \langle + | \rho(1,1) | + \rangle - \langle - | \rho(0,0) | - \rangle - \langle - | \rho(1,1) | - \rangle ,$$

because the higher photon states are neglected. The result has the general form

$$\Delta p = -\frac{1-F/H}{1+G/H} , \tag{4.5}$$

where

$$H = \left[g^2 \left[\kappa + 4\beta^2 \frac{1-\gamma/\gamma_e}{\gamma+2\kappa} \right] + \frac{\gamma D}{2} \right] \times \left[g^2 \left[\frac{\gamma}{2} + \kappa + \frac{g^2}{\kappa} \right] + \frac{\gamma D}{2} \right] , \tag{4.5a}$$

$$F = 2g^2\beta^2(D-g^2) \left[1 - \frac{\gamma}{\gamma_e} \left[2 - \frac{\gamma_e - \gamma}{\kappa} \right] \right] , \tag{4.5b}$$

$$G = 2\beta^2(D-g^2) \left[D - g^2 + \frac{g^2\gamma}{\gamma_e} \left[2 - \frac{\gamma_e - \gamma}{\kappa} \right] \right] , \tag{4.5c}$$

and where

$$\gamma_e = \gamma + \kappa + 2\frac{g^2(\gamma+2\kappa)}{(\gamma+2\kappa)(\gamma+4\kappa)+8\beta^2} , \tag{4.6}$$

$$D = \left[\frac{\gamma}{2} + \kappa + \frac{g^2}{\kappa} \right] \left[\kappa + 4\beta^2 \frac{1-\gamma/\gamma_e}{\gamma+2\kappa} \right] + 2\beta^2 \left[1 - \frac{\gamma}{\gamma_e} \left[2 - \frac{\gamma_e - \gamma}{\kappa} \right] \right] . \tag{4.7}$$

Equations (4.5), though complete, do not show us the structure of the result. The simplest possible approximation that still contains the inversion is the neglect of the spontaneous emission by setting $\gamma = 0$. In addition, we have already assumed that $g \ll \kappa$. This gives us the result

$$\Delta p \cong -\frac{1 - \dfrac{2\beta^2(\kappa^2+4\beta^2)}{g^2(\kappa^2+2\beta^2)}}{1 + \dfrac{2\beta^2(\kappa^2+4\beta^2)^2}{g^4(\kappa^2+2\beta^2)}} . \tag{4.8}$$

We see that the inversion is positive when $\beta > g/\sqrt{2}$ and continues to be positive when β increases. In the limit $\beta \to \infty$, Δp approaches zero from the positive side. The behavior of Δp is shown in Fig. 7. Note that the result of Eq. (4.8) is more general than that given by the straightforward perturbation expansion, which would be obtained by taking the limit $g \to 0$ and keeping the lowest-order term. The perturbative result would give the wrong small-intensity behavior because it assumes that g is the smallest of the parameters and hence also smaller than β. The order of the limiting processes near a singular point is not interchangeable. As mentioned, the system has a cavity induced spontaneous emission process

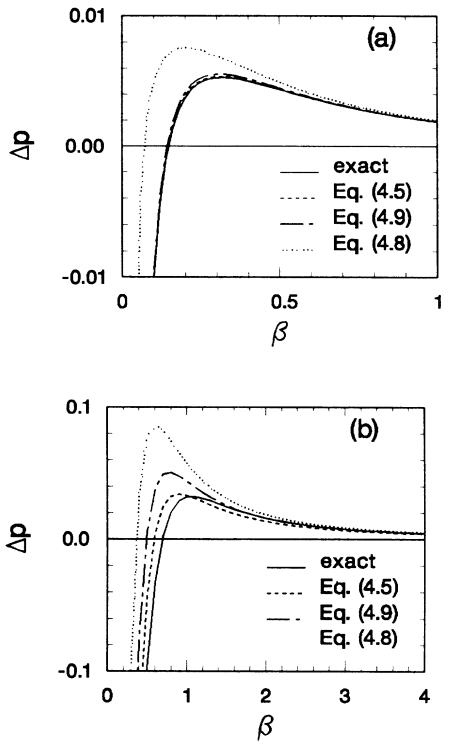

FIG. 7. Graphs of the inversion Δp vs driving field $\beta = gE/\kappa$ as given by various analytic approximations. The solid curve is the exact numerical result. The other curves are various analytic approximations discussed in Sec. IV A. (a) Parameters: $C = 0.5$, $n_s = 0.005$ ($g/\kappa = 0.1$, $\gamma/\kappa = 0.02$). The approximations of Eqs. (4.5) and (4.9) almost coincide with the exact result. (b) Parameters: $C = 2$, $n_s = 0.01$ ($g/\kappa = 0.57$, $\gamma/\kappa = 0.16$). The agreement is not as good as in case (a) because g is now larger.

which vanishes when $g \to 0$. With vanishing damping the inversion reaches zero value with any finite field. However, with any finite damping the inversion goes towards $\Delta p = -1$ with vanishing field β. This behavior is familiar also from semiclassical two-level systems.

From Eq. (4.8) we see that when $\beta \cong \sqrt{g\kappa}$ we have $\Delta p \cong g^2/\kappa^2$ and when $\beta \gg \kappa$ we obtain $\Delta p \cong g^2/4\beta^2$. In the current approximation the inversion has a maximum value of the order g^2/κ^2. Our assumptions of the relative sizes of the parameters demand that the inversion be small. In Sec. III we numerically showed that by increasing the ratio g/κ we cannot increase the maximum inversion beyond the value 0.07. The positive inversion is always small. For the multimode case, discussed near the end of Sec. II, the threshold of positive inversion shifts to higher fields (by a factor of $N_m^{1/4}$) according to the scaling of Eq. (2.9). Also, the inversion at the maximum is increased N_m times. However, the maximum inversion obtainable does not change because it is obtained optimizing the coupling constant g. The maximum value is obtained in a region where our approximate analytic result, and consequently conclusions drawn from it are not valid.

To obtain Eq. (4.8) the spontaneous emission was completely neglected. We now use Eqs. (4.5) to see how the

spontaneous emission influences the inversion. We assume that g and γ are small but finite, which gives us a result of the form Eq. (4.5),

$$\Delta p = -\frac{1-F/H}{1+G/H} , \tag{4.9}$$

where now

$$H = \left[\frac{g^2}{\kappa}(\kappa^2+2\beta^2)+\frac{\gamma}{2}(\kappa^2+4\beta^2)\right] \times \left[g^2\kappa+\frac{\gamma}{2}(\kappa^2+4\beta^2)\right] , \tag{4.9a}$$

$$F = 2\beta^2 g^2(\kappa^2+4\beta^2) , \tag{4.9b}$$

$$G = 2\beta^2(\kappa^2+4\beta^2)^2 . \tag{4.9c}$$

As expected, increasing the spontaneous emission uniformly decreases the inversion. In Fig. 7 we compare the approximate result Eq. (4.9) with exact numerical results and at the same time show that the spontaneous emission decreases the inversion. If we have $\gamma \geq \sqrt{2}g$, then the inversion can no longer be positive and the effect disappears. If the buildup of coherence between different photon states is prohibited by the spontaneous emission, the quantum effects are unimportant and positive inversion cannot occur.

B. Approach to steady state

From the experimental point of view it is important to know how fast the system reaches the steady state. We again completely neglect the spontaneous emission by assuming γ to be the slowest rate. The system has a natural rate κ for cascading down the photon ladder. However, in the absence of spontaneous emission the cavity damping alone is not able to bring the system into steady state. It cannot relax the state $|0,+\rangle$ down to $|0,-\rangle$ and consequently the Rabi oscillations in the zero photon state are not damped. The quantum-mechanical coupling between states $|0,+\rangle$ and $|1,-\rangle$, measured by g, provides a way to incoherently connect the state $|0,+\rangle$ to $|0,-\rangle$ because the state $|1,-\rangle$ decays due to the cavity losses to $|0,-\rangle$. The rate is estimated by g^2/κ using Fermi's golden rule; g is the interaction matrix element and κ is the effective width of the intermediate state $|1,-\rangle$. This rate is much smaller than the cavity damping rate κ, so the time in which the system reaches the steady state is considerably longer than κ^{-1}. Also, for large photon numbers n the rate is, as a spontaneous emission rate should be, essentially independent of n because $g \to \sqrt{n}\,g$, and $\kappa \to n\kappa$.

To get quantitative results about the rates we solve the eigenvalue problem determined by Eqs. (4.1)–(4.4). The smallest eigenvalues give the inverse time scales for reaching the steady state. In general this leads to a 16-dimensional eigenvalue determinant. However, in the limit $g \ll \kappa$ we can reduce the system by introducing a suitable linear combination of the equations. We write the equations with $\rho(0,0)+\rho(1,1)$ and $\rho(1,1)$ as the independent variables. Because of the weak coupling the contribution of $\rho(1,1)$ can be neglected. The remaining problem is 12 dimensional, but can be evaluated. The resulting eigenvalue equation is

$$\lambda(\lambda+\kappa)^3\{\lambda[(\lambda+\kappa)^2+4\beta^2]+g^2(\lambda+\kappa)\}\{[(\lambda+\kappa)(\lambda^2+4\beta^2)+\lambda g^2][(\lambda+\kappa)^2+4\beta^2]+2g^2(\lambda+\kappa)[\lambda(\lambda+\kappa)+g^2-4\beta^2]\}=0 . \tag{4.10}$$

The eigenvalue zero corresponds to the steady state. We are not interested in the eight eigenvalues of the order of κ but instead only in the three with real part of the order g^2/κ. The first eigenvalue is

$$\lambda \cong -\frac{g^2\kappa}{\kappa^2+4\beta^2} ,$$

corresponding to damping of the off phase or the imaginary part of the polarization; the second constant of motion in a two-level system in exact resonance. We notice that the damping rate decreases with increasing external field. The remaining two eigenvalues correspond to the damping of the Rabi oscillations. With finite g one has to separately consider the case β small and β large. If β is large we obtain the approximate eigenvalue

$$\lambda \cong i2\beta - \frac{g^2}{2(\kappa+i2\beta)} - \frac{g^2}{\kappa}$$

and its complex conjugate. When β is small the eigenvalues are purely real and we have

$$\lambda \cong -\frac{2g^2}{\kappa}, -\frac{g^2}{\kappa} .$$

The Rabi oscillations relax essentially with the rate g^2/κ as expected but the off-phase polarization can decay more slowly, like $g^2\kappa/4\beta^2$, with high Rabi frequencies. The eigenvalues obtained show how the cavity has enhanced the spontaneous emission.[5] The quantum-mechanical field coupling provides additional decay routes increasing the total decay rate (Sec. II) from the (here neglected) value γ. Additionally these eigenvalues determine the positions and widths of the peaks of the resonance fluorescence spectrum. Hence, we predict a triplet of peaks the widths of which get narrower with increasing external field β. This is in accordance with the results of Lewenstein *et al.*[4]

V. CONNECTION TO THE WEISSKOPF-WIGNER THEORY OF SPONTANEOUS EMISSION

In this section we relate the positive inversion to modifications of mode couplings in the context of the commonly used Weisskopf-Wigner theory of spontaneous emission. As noted earlier strong cavity damping cascades the quantum part of the resonant mode to low photon numbers and therefore makes the spontaneous pro-

cesses important. In this case the model becomes equivalent to the one used when we study the spontaneous emission in the presence of a strong semiclassical mode. However, the coupling coefficients are modified by the resonant cavity in comparison to the pure vacuum case. To discover the origin of the positive inversion and what conditions must be satisfied to obtain it we work through the Weisskopf-Wigner theory in a generalized form.[19]

That part of the density-matrix equation representing coupling to the quantum field modes is given by

$$L_{\rm af}(\rho)=\sum_{\lambda} g(\lambda)[a_{\lambda}^{\dagger}\sigma_{-}-a_{\lambda}\sigma_{+},\rho] , \tag{5.1}$$

where the sum is over all field modes. The model studied in previous sections is regained by setting $g(\lambda)$ equal to a δ function. We include the interaction with the semiclassical field in the atomic part of the equation of motion and the free photon Hamiltonian is included in L_f. We restrict ourselves to the case of the atom being in exact resonance with the driving field. Then

$$\begin{aligned} L_a(\rho)&=[\beta(\sigma_{-}-\sigma_{+}),\rho] , \\ L_f(\rho)&=-i\sum_{\lambda}\Omega_{\lambda}[a_{\lambda}^{\dagger}a_{\lambda},\rho] , \end{aligned} \tag{5.2}$$

where Ω_{λ} is the detuning between the atomic transition and the mode λ. Cavity damping is introduced later and included in the adiabatic damping parameter.

We look for the equation of motion for the reduced density matrix ρ_r, obtained by tracing over the field,

$$\rho_r=\mathrm{tr}_f(\rho) .$$

The equation of motion for ρ_r is then

$$\frac{d}{dt}\rho_r=L_a(\rho_r)+\mathrm{tr}_f(L_{\rm af}(\rho)) . \tag{5.3}$$

The first term on the right-hand side of Eq. (5.3) describes the interaction with the semiclassical field and the second term the interaction with the quantum field. The second term can be written in the form

$$\begin{aligned} \mathrm{tr}_f(L_{\rm af}(\rho))=\sum_{\lambda} g(\lambda)\{&[\sigma_{-},\mathrm{tr}_f(a_{\lambda}^{\dagger}\rho)] \\ &-[\sigma_{+},\mathrm{tr}_f(a_{\lambda}\rho)]\} . \end{aligned} \tag{5.4}$$

By neglecting the higher off-diagonal density-matrix elements of the photon states and the coherences between different modes we obtain the equation of motion

$$\begin{aligned} \frac{d}{dt}\mathrm{tr}_f(a_{\lambda}\rho)=&(L_a-i\Omega_{\lambda})[\mathrm{tr}_f(a_{\lambda}\rho)] \\ &+g(\lambda)[\sigma_{-}\,\mathrm{tr}_f(a_{\lambda}a_{\lambda}^{\dagger}\rho) \\ &-\mathrm{tr}_f(a_{\lambda}^{\dagger}a_{\lambda}\rho)\sigma_{+}] . \end{aligned} \tag{5.5}$$

The modes are practically empty so we get

$$\sigma_{-}\,\mathrm{tr}_f(a_{\lambda}a_{\lambda}^{\dagger}\rho)-\mathrm{tr}_f(a_{\lambda}^{\dagger}a_{\lambda}\rho)\sigma_{+}\cong\sigma_{-}\rho_r .$$

We adiabatically eliminate $\mathrm{tr}_f(a_{\lambda}\rho)$ by inserting a damping rate and taking the steady state of Eq. (5.5). So we write

$$\frac{d}{dt}\mathrm{tr}_f(a_{\lambda}\rho)\rightarrow\eta_{\lambda}\,\mathrm{tr}_f(a_{\lambda}\rho) .$$

Here η_{λ} can describe either cavity damping or damping by the continuum of vacuum modes. We obtain the equation

$$(L_a-i\Omega_{\lambda}-\eta_{\lambda})[\mathrm{tr}_f(a_{\lambda}\rho)]=-g(\lambda)\sigma_{-}\rho_r . \tag{5.6}$$

A similar equation is obtained for $\mathrm{tr}_f(a_{\lambda}^{\dagger}\rho)$. We do not go into the details of inverting Eq. (5.6) because it is straightforward.[20] After inserting the result in Eqs. (5.3)–(5.4) we obtain the equations of motion

$$\begin{aligned} \frac{d}{dt}\langle\sigma_{-}\rangle&=\beta\langle\Delta\hat{p}\rangle-\tfrac{1}{2}(\alpha_{+}+\alpha_{-})\langle\sigma_{-}\rangle \\ &\quad+\tfrac{1}{2}i(\alpha_{+}-\alpha_{-})\langle\sigma_{+}\sigma_{-}\rangle , \\ \langle\sigma_{+}\rangle&=\langle\sigma_{-}\rangle^{*} , \\ \frac{d}{dt}\langle\Delta\hat{p}\rangle&=-2\,\mathrm{Re}\{[2\beta+\tfrac{1}{2}i(\alpha_{+}-\alpha_{-})]\langle\sigma_{-}\rangle\} \\ &\quad-\mathrm{Re}(2\alpha_0+\alpha_{+}+\alpha_{-})\langle\sigma_{+}\sigma_{-}\rangle , \end{aligned} \tag{5.7}$$

where the coefficients α are given by

$$\begin{aligned} \alpha_0&=\sum_{\lambda} g(\lambda)^2\frac{1}{\eta+i\Omega_{\lambda}} , \\ \alpha_{\pm}&=\sum_{\lambda} g(\lambda)^2\frac{1}{\eta+i(\Omega_{\lambda}\mp 2\beta)} . \end{aligned}$$

Equations (5.7) have the familiar damping terms except that they are modified by the driving field. In the pure vacuum case these modifications vanish because of the broad density of states and structureless coupling coefficient. If the coupling constant has structure, the spontaneous emission can be considerably changed. This leads, for example, to the cavity-enhanced spontaneous emission discussed earlier. In addition to the damping and the Lamb-shift-type terms we have also introduced new coupling between $\langle\Delta\hat{p}\rangle$ and $\langle\sigma_{-}\rangle$. In the pure vacuum case this coupling vanishes because of its dispersive nature, which causes the integral over frequencies to average to zero. However, when some modes are privileged, the coupling measured by

$$i\frac{\alpha_{+}-\alpha_{-}}{2}$$

may be nonzero and may even be dominant if the ordinary spontaneous emission to vacuum modes is small.

From Eq. (5.7) we see that if the system is saturated due to the external field and if the spontaneous emission is negligible the steady-state inversion is given by

$$\langle\Delta\hat{p}\rangle\cong\mathrm{Im}\frac{\alpha_{+}-\alpha_{-}}{2\beta} , \tag{5.8}$$

because $\langle\sigma_{-}\rangle\cong 0$ and $\langle\sigma_{+}\sigma_{-}\rangle\cong\frac{1}{2}$. In our case, when only one mode has a dominant effect and is in resonance with the external field, the result, inserting α's, is

$$\langle\Delta\hat{p}\rangle\cong\frac{g^2}{\eta^2+4\beta^2} . \tag{5.9}$$

The inversion is positive. This result can be obtained from Eq. (4.5) in the strong-field limit after setting $\eta=\kappa$. In the multimode case the inversion is additive as long as this approximation is valid and we stay at small photon numbers and can neglect the coherences between different modes; but is not additive in general.

VI. EXPERIMENTAL CONSIDERATIONS

This section considers equations which arise when one asks how steady-state inversion might be considered in the laboratory. We first suggest experimental signatures of positive inversion and then discuss the conditions necessary for its realization.

In semiclassical theory population inversion is associated with gain. One may then look for inversion by seeking gain on a probe beam or by attempting laser oscillation with the inverted atoms as the laser medium. But steady-state positive inversion is possible only because semiclassical theory fails. So we cannot rely on its prediction of gain from our inverted medium.

The correct quantum-mechanical treatment of a probe beam interacting with our atom in a cavity is a three-wave mixing problem, which is an interesting subject for further research. Preliminary work suggests the absence of a semiclassical type of association of population inversion and gain in our system.

We discuss two signatures of the positive inversion in the atomic fluorescence. First consider an experiment such as performed by Heinzen, Childs, Thomas, and Feld[2] on cavity-enhanced spontaneous emission. The atom is driven by a laser from outside the cavity. The cavity is then blocked and unblocked, modifying the structure of the electromagnetic vacuum seen by the atom. Heinzen *et al.*[2] found a fluorescence decrease on unblocking the cavity. On the contrary, for our conditions (small-, high-finesse cavity), we predict a fluorescence increase when the cavity is unblocked. This is because the fluorescence is proportional to the excited state population,[21] which is increased by the coupling to the cavity. In the original experiment of Heinzen *et al.*[2] cavity-enhanced spontaneous emission depopulated the excited state and the fluorescence decreased.

Figure 3 illustrates the second signature. As the driving field increases from zero the inversion passes through a maximum, and then saturates to zero. So the fluorescence out the side of the cavity will also have a maximum and subsequent decrease as the driving field is increased from zero. This maximum in the fluorescence is a signature of positive inversion. When positive inversion does not occur the fluorescence has no maximum and the atom saturates to zero inversion from below. This fluorescence maximum is a small effect; for a maximum inversion of $\Delta p=0.01$ the maximum fluorescence intensity exceeds the large field saturation value by 1%.

Having found signatures of positive inversion we next consider the requirements for achieving it. The work of Sec. III (Fig. 4) showed that population inversion requires a small saturation photon number, $n_s \ll 1$, and a large C. Small n_s corresponds to a small number of photons producing an electric field at the atom sufficient to saturate the transition. In practice this is achieved using a tightly focused Gaussian cavity mode. The atom is placed in the strong electric field at the beam waist. A large C is achieved with a high-finesse cavity and ensures that the field-atom feedback is strong.

How can we ensure that the steady state has been reached? One needs to clearly distinguish it from the transient inversion due to Rabi oscillations, for example. From this point of view an ion trap or very slow atomic beam is desirable.[22] A related difficulty is the variation of the atom-field coupling constant g with position in the cavity mode, Eq. (2.2a). Lack of atomic localization implies that the fluorescence maximum will be washed out by the variation in the optimum driving field with g; see, for example, Eq. (4.8). Because of this a ring cavity is preferable to a standing wave Fabry-Perot, in which g varies from zero to its maximum over half a wavelength of longitudinal distance. In contrast a ring cavity might only require localization to a few wavelengths in the transverse direction.

Figure 8 shows the inversion as a function of time. At time zero a ground state atom was injected into the empty, but driven, cavity. Therefore the initial state was an unexcited atom and cavity mode in the coherent state, $|-\rangle\otimes|E/\kappa\rangle$. The figure shows damped Rabi oscillations in accordance with the discussion of Sec. IV. How long must the atom remain in the beam before it reaches steady state? For the parameters of Fig. 8 ($C=2$, $n_s=0.01$) about 15 cavity lifetimes or $15/(4\times10^8)\cong40$ ns are required. This is the time the atom (or ion) must remain in the beam waist for steady-state inversion to be achieved. For a beam experiment this yields an upper limit on the beam velocity of $v_{\max}\cong 2w_0/40$ ns. For sodium and a beam waist of ten wavelengths $v_{\max}\cong 300\ \mathrm{ms}^{-1}$. For a beam waist of five wavelengths $v_{\max}\cong 150\ \mathrm{ms}^{-1}$.

As a quantitative example we use the sodium D transition, which has angular frequency $\omega\cong 3.4\times10^{15}\ \mathrm{s}^{-1}$ and spontaneous emission rate (Einstein-A coefficient) $\gamma\cong 6.3\times10^7\ \mathrm{s}^{-1}$. We approximate a ring cavity mode by the Gaussian mode function,[23]

$$|u(\mathbf{r})|=[\tfrac{1}{2}\pi L w(z)^2]^{-1/2}\exp[-r^2/w(z)]\ , \qquad (6.1)$$

where L is the cavity length, $w(z)$ is the beam radius at

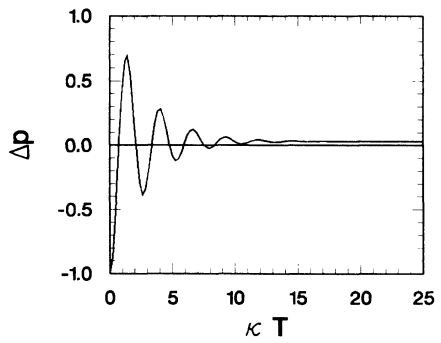

FIG. 8. Graph of the inversion vs time showing damped Rabi oscillations. At time zero the state was the field in the coherent state of amplitude E/κ and the atom in the ground state. Time is in units of the inverse cavity damping time κ^{-1}. Parameters: $C=2$, $n_s=0.01$, $Y=20$ ($g/\kappa=0.57$, $\gamma/\kappa=0.16$, $E/\kappa=2$).

longitudinal coordinate z, and r is the transverse radial coordinate. Assuming the atom to be localized at the beam waist, $w(0)=w_0$, and taking $r=0$ Eq. (2.2a) yields

$$g^2=\left[\frac{3\pi\gamma c^3}{2\omega^2}\right]|u|^2\cong(1.4\times10^{15})L^{-1}(w_0/\lambda)^{-2}\ . \tag{6.2}$$

Then from Eq. (2.15)

$$n_s=(0.35)L(w_0/\lambda)^2\ , \tag{6.3a}$$

$$C=(0.047)F(w_0/\lambda)^{-2}\ , \tag{6.3b}$$

where we have introduced the cavity finesse $F=\pi c/2L\kappa$. Inverting Eqs. (6.3) we find

$$L=(2.9)(w_0/\lambda)^{-2}n_s,\quad F=(21)(w_0/\lambda)^2C\ . \tag{6.4}$$

Therefore a small n_s corresponds to a short cavity length and a high C implies high cavity finesse. With a beam waist of ten wavelengths Eqs. (6.4) become

$$L=(0.03)n_s\ \text{(meters)},\quad F=(2100)C\ . \tag{6.5}$$

For example, a Y maximized inversion of $\Delta p=0.01$, obtained with $n_s=0.04$ and $C=0.5$, implies $L=1.2$ mm and $F=1000$. A smaller beam waist lowers the required finesse and increases the required cavity length. For example, with a beam waist of five wavelengths, $L=4.8$ mm and $F=250$. The preceding parameter estimates are more favorable than those of Ref. 1. There the mode was assumed to be plane wave with volume πw_0^2L, which reduces the maximum coupling g.

In conclusion we find no fundamental technological obstacles to observing steady-state positive inversion. However, a combination of atomic beam slowing and/or ion trapping technologies with state-of-the-art cavities seems desirable.

VII. SUMMARY

We have studied the occurrence of population inversion in a driven two-level atom in a cavity. The semiclassical prediction that a two-level transition cannot be inverted in steady state by a coherent driving field is violated. The inversion is a consequence of large quantum fluctuations in that it does not follow from the usual linearized treatment of quantum fluctuations.

Our mathematical model of the driven, dissipative atom-field system contains all of its essential elements. We have given various analytic approximations which show the inversion and agree well with the "exact" numerical solutions in appropriate limits. As a function of driving field the inversion reaches its maximum soon after becoming positive. Thereafter the inversion decreases to zero for large driving fields. This qualitative effect is a signature of steady-state inversion.

Numerically we have demonstrated that the inversion in our system cannot exceed a certain small value; $\Delta p\lesssim0.07$. If more than one atom is interacting with the cavity mode the inversion per atom slowly decreases as the number of atoms increases. If the atom is (equally) coupled to more than one cavity mode it behaves as if coupled to a single mode but with an enhanced coupling constant g.

We have placed the positive inversion result in the context of enhanced and inhibited spontaneous emission[2,3] by explicitly considering the Weisskopf-Wigner spontaneous emission theory in the presence of a resonant cavity. The discrete mode structure of the cavity, in contrast to the vacuum's continuum, allows positive inversion in addition to cavity-enhanced spontaneous emission.

Investigation of the experimental requirements for positive inversion gave encouraging results. At least two approaches are possible. The Heinzen *et al.*[2] setup, in which the cavity is alternately blocked and unblocked, or a search for a fluorescence maximum as a function of driving field. An important consideration is whether the atoms remain in the beam waist long enough to have reached the steady state. The required cavities are small (millimeters) and high finesse ($F\cong500$).

Reference 1 gave a simple explanation of the steady-state inversion. This involved atomic polarization transport into the ground field state leading to population transport into the excited atomic state. The explanation depended on cavity damping, which is consistent with the view that the inversion is a result of vacuum modification by the cavity. We have not found any coherences, which, without losing the inversion, could be neglected in order to obtain a simpler explanation of the inversion. This suggests that the details of the inversion are subtlely dependent on the entire system dynamics.

Steady-state positive inversion provides a possibility to test our commonly used model for a single atom interacting with the electromagnetic field in the presence of a resonant cavity.

ACKNOWLEDGMENTS

The authors acknowledge conversations with H. J. Carmichael, T. A. B. Kennedy, P. Meystre, and E. Wright. This work was supported by the Office for Naval Research and by the National Science Foundation Grant No. PHY-86-03368.

[1]C. M. Savage, Phys. Rev. Lett. **60**, 1828 (1988).

[2]D. J. Heinzen, J. J. Childs, J. E. Thomas, and M. S. Feld, Phys. Rev. Lett. **58**, 1320 (1987); E. M. Purcell, Phys. Rev. **69**, 681 (1946).

[3]W. Jhe, A. Anderson, E. A. Hinds, D. Meschede, L. Moi, and S. Haroche, Phys. Rev. Lett. **58**, 666 (1987).

[4]M. Lewenstein, T. W. Mossberg, and R. J. Glauber, Phys. Rev. Lett. **59**, 775 (1987); M. Lewenstein and T. W. Mossberg, Phys. Rev. A **37**, 2048 (1988).

[5]P. Rice and H. J. Carmichael, IEEE, J. Quantum Electron. **24**, 1351 (1988).

[6]C. M. Savage and H. J. Carmichael, IEEE J. Quantum Electron. **24**, 1495 (1988).

[7]See articles by H. J. Kimble and by H. J. Carmichael, in E. R.

Pike and S. Sarkar, *Frontiers in Quantum Optics* (Adam Hilger, Bristol, 1986).

[8]See the special issue on squeezed light, J. Opt. Soc. Am. B **4** (1987); see the special issue on squeezed light, J. Mod. Opt. **34** (1987).

[9]H. J. Carmichael and D. F. Walls, J. Phys. B **9**, L43 (1976); H. J. Kimble, M. Dagenais, and L. Mandel, Phys. Rev. Lett. **39**, 691 (1977).

[10]C. W. Gardiner, *Handbook of Stochastic Methods* (Springer-Verlag, Berlin, 1985).

[11]P. D. Drummond and D. F. Walls, Phys. Rev. A **23**, 2563 (1981).

[12]J. H. Eberly, N. B. Narozhny, and J. J. Sanchez-Mondragon, Phys. Rev. Lett. **44**, 1323 (1980); G. Rempe, H. Walther, and N. Klein, *ibid.* **58**, 353 (1987).

[13]B. Yurke and D. Stoler, Phys. Rev. Lett. **57**, 13 (1986).

[14]T. A. B. Kennedy and P. D. Drummond, Phys. Rev. A **38**, 1319 (1988).

[15]M. Wolinsky and H. J. Carmichael, Phys. Rev. Lett. **60**, 1836 (1988).

[16]D. T. Pegg, *Laser Physics, Proceedings of the Second New Zealand Summer School in Laser Physics,* edited by D. F. Walls and J. D. Harvey (Academic, Sydney, 1980).

[17]S. Sarkar and J. S. Satchell, J. Phys. A **20**, 2147 (1987).

[18]A. M. Smith and C. W. Gardiner, Phys. Rev. A **38**, 4073 (1988).

[19]See, for example, S. Stenholm, *Foundations of Laser Spectroscopy* (Wiley, New York, 1984), pp. 227–255; C. Cohen-Tannoudji, in *Frontiers in Laser Spectroscopy,* Les Houches Summer School 1975, edited by R. Balian, S. Haroche, and S. Liberman (North-Holland, Amsterdam, 1975).

[20]A. Messiah, *Quantum Mechanics* (North-Holland, Amsterdam, 1966), Vol. II, Chap. 16.III.

[21]H. J. Kimble and L. Mandel, Phys. Rev. A **13**, 2123 (1976).

[22]J. Prodan *et al.,* Phys. Rev. Lett. **54**, 992 (1985); W. Ertmer *et al., ibid.* **54**, 996 (1985).

[23]P. D. Drummond, IEEE J. Quantum Electron. **17**, 301 (1981); A. E. Siegman, *Lasers* (University Science Books, Mill Valley, 1986).